Hindawi Publishing Corporation
International Journal of Photoenergy
Volume 2013, Article ID 130541, 7 pages
http://dx.doi.org/10.1155/2013/130541

Research Article

Annealing Effect of ZnO Seed Layer on Enhancing Photocatalytic Activity of ZnO/TiO_2 Nanostructure

Woo-Young Kim,[1] Soon-Wook Kim,[1] Dae-Hwang Yoo,[1,2] Eui Jung Kim,[3] and Sung Hong Hahn[1,2]

[1] *Department of Physics, University of Ulsan, Ulsan 680-749, Republic of Korea*
[2] *Basic Science Research Institute (Energy Harvest-Storage Research Center), University of Ulsan, Ulsan 680-749, Republic of Korea*
[3] *Department of Chemical Engineering, University of Ulsan, Ulsan 680-749, Republic of Korea*

Correspondence should be addressed to Sung Hong Hahn; shhahn@ulsan.ac.kr

Received 14 March 2013; Accepted 26 April 2013

Academic Editor: David Lee Phillips

Zinc oxide (ZnO)/titanium dioxide (TiO_2) nanorods have been synthesized via a hydrothermal method for ZnO nanorods and an electron-beam deposition for TiO_2 nanorods. This work examined the effect of annealing ZnO seed layer on the photocatalytic activity of the ZnO/TiO_2 nanorods which was determined from photodecomposition of methylene blue under UV irradiation. The photocatalytic activity of the ZnO/TiO_2 nanorods was improved with increasing annealing temperature of the seed layer from 300°C to 500°C. Annealing the seed layer at 500°C showed the best photocatalytic activity resulting from high UV absorption ability, a large surface area with flower structure and copious oxygen defects which promote separation of electron-hole pairs reducing electron recombination. The prepared nanorods were characterized by field emission-scanning electron microscopy (FE-SEM), X-ray diffraction (XRD), photoluminescence (PL), and UV-visible spectroscopy.

1. Introduction

The synthesis of semiconductor nanomaterial is of great worldwide interest. The nanomaterials have enhanced optical and electronic properties, finding their application in various fields such as optoelectronic nanodevices and optical excitations [1–3]. Titanium dioxide (TiO_2) is the most promising material for a photocatalyst, because it has good photoactivity, long-term stability, and low cost. Anatase phase, one of TiO_2 crystal structures, shows higher photoactivity than rutile [4, 5]. Zinc oxide (ZnO), which has a direct band gap of 3.37 eV and large exciton binding energy of 60 meV, has a high mechanical and a thermal stability [6–8]. In addition, it can be utilized as a source which makes blue/UV optoelectronic devices due to its photochemical properties [9]. It is known that ZnO/TiO_2 nanomaterials promote charge separation decreasing electron-hole recombination [10]. Furthermore, they have high chemical and thermal stability and high absorption in the UV region [11]. As a result, the ZnO/TiO_2 nanorods show an enhanced photocatalytic activity. The fabrication of one-dimensional (1D) nanostructures has attracted considerable attention due to their great optical and electrical properties [12]. Various 1D of ZnO nanostructures such as nanorods, nanowires, and nanorings have been synthesized by physical and chemical methods including molecular beam epitaxy (MBE) [13], plasma-enhanced chemical vapor deposition (PECVD) [14], thermal evaporation [15], and template based method [16]. The wet chemical processes are a cost-effective low-temperature technique [17–20]. The hydrothermal technique is an effective method to control the 1D ZnO nanostructure [21], which is surface independent [22]. The physical properties of the ZnO/TiO_2 nanorods relate to their nanostructure which is dependent on deposition conditions and annealing. Especially, the annealing of the ZnO seed layer improved adhesion on substrate, which contributed to well-aligned ZnO nanorods [23]. The annealing process is important to obtain desirable structural and optical properties. The main contributions

of seed layer annealing may come from the improvement of the crystallinity and absorption which could give an significantly effect on the photocatalytic acitivity of ZnO/TiO_2 nanorods [24].

In this study, we investigate the effect of seed layer annealing of the ZnO/TiO_2 nanorods on the photocatalytic activity. The TiO_2 nanorods were prepared by electron-beam evaporation. ZnO seed solution was then spin-coated on the TiO_2 nanorods, which was followed by annealing at 300°C, 400°C, and 500°C. Subsequently, the ZnO nanorods have been grown by hydrothermal method.

2. Experiments

2.1. Preparation of TiO_2 Nanorods. TiO_2 nanorods were obliquely deposited on quartz substrate using electron-beam evaporation. TiO_2 tablets with high purity (99.99%) were used as a raw material. After the deposition chamber was evacuated to a base pressure of 6×10^{-6} torr, the TiO_2 films were deposited at a working oxygen gas pressure of 5×10^{-5} torr. The working current was 200 mA and the electron gun voltage was 7.0 kV. The electron beam was irradiated at an incident angle of 75° to obtain the TiO_2 nanorods. The prepared nanorods were annealed at 600°C for 1 hour to form anatase structure.

2.2. Growth of ZnO Nanorods. ZnO nanorods were grown on the prepared TiO_2 nanorods via a hydrothermal method. ZnO seed solution was prepared by dissolving 5 mM of zinc acetate dihydrate ($C_4H_6O_4Zn{\cdot}2H_2O$) in 100 mL of methoxy ethanol and then stirring for 24 hours. The ZnO seed solution was spin-coated on the TiO_2 nanorods/quartz substrate twice. The ZnO seed coated sample was annealed at 300°C, 400°C, and 500°C, which are referred to as ZT-300, ZT-400, and ZT-500, respectively. The ZnO growth solution was prepared by dissolving 16 mM of zinc nitrate hexahydrate ($Zn(NO_3)_2{\cdot}6H_2O$) and 25 mM of hexamethylenetetramine (HMT) into 200 mL of distilled water. The ZnO seed coated sample was immersed into the growth solution at 90°C for 4 hours. The sample was then removed from the solution, washed with distilled water, and annealed at 350°C for 1 hour. For comparison, ZnO nanorods were grown without TiO_2, and their seed layers were annealed at 300°C, 400°C, and 500°C, which are labeled as Z-300, Z-400, and Z-500, respectively.

2.3. Characterization and Photocatalytic Activity. The surface morphology of the ZnO/TiO_2 and TiO_2 nanorods was examined by field emission-scanning electron microscopy (FE-SEM, Supra 40, Carl Zeiss, Swiss). The X-ray diffraction (XRD) patterns were measured with a Rint 2000 vertical goniometer using Cu Kα radiation at 40 kV and 100 mA. The photoluminescence (PL) was measured by a SPEX 750 M PL spectrometer with 325 nm He-Cd laser with 4 mW output power at room temperature. UV-vis absorbance spectra were examined to investigate absorption property of the ZnO/TiO_2 nanorods. The photocatalytic activities of the ZnO/TiO_2 and ZnO nanorods were examined using a UV-visible spectrophotometer (HP 8453) by measuring the photodegradation rate of methylene blue (MB) with an initial concentration of 1×10^{-5} mol/L. The thin films were immersed in the MB solution in a tubular quartz reactor under four surrounding UV lamps of 20 W (wavelength = 352 nm). After dark adsorption equilibrium for 30 min, photodegradation of the MB was measured by UV-vis spectrophotometer (HP 8453) at λ_{max} = 664 nm.

3. Results and Discussion

Figure 1 shows the SEM images of TiO_2 nanorods (as the buffer layer), ZT-300, ZT-400, and ZT-500. The obliquely deposited TiO_2 nanorod arrays have a high surface area as shown in Figure 1(a). Figure 1 observed that the size and structure of the ZnO nanorods depend on the annealing temperature of the seed layer. From the SEM results, the sizes of the TiO_2 nanorods and ZT-300, ZT-400, and ZT-500 were evaluated to diameter with (a) 21.1 nm, (b) 306.8 nm, (c) 210.2 nm, and (d) 96.6 nm, and length with (e) 60.0 nm, (f) 2.98 μm, (g) 2.48 μm, and (h) 1.91 μm. In the case of ZT-500, a flower-like structure composed of thin nanorods was formed, which relates to the polycrystalline structure of the large-size ZnO seed as shown in Figure 1(c). The big grains are polycrystalline ZnO seeds consisting of plenty of small crystallites [24]. The ZnO nanorods have been grown on the TiO_2 nanorod arrays with a porous surface. As a result, the agglomerate of ZnO nanorods with various directions was formed [19].

Figure 2 displays the XRD patterns of the Z-300, ZT-300, ZT-400, and ZT-500. In case of the ZnO (JCPDS card no. 79-2205) nanorods, the (100), (002), (101), and (102) peaks appeared. The high intensity (002) peak indicates that the prepared ZnO nanorods have hexagonal wurtzite structure and are grown along the *c*-axis direction to the substrate surface [25, 26]. With the increase of the seed annealing temperature, the intensity of the (002) peak decreased due to a decrease in the reinforced atomic diffusion between the ZnO and TiO_2. When the seed layer of the ZnO/TiO_2 nanorods was annealed at high temperature, the atoms can acquire energy enough to move, leading to strengthened interdiffusion motion between the ZnO and TiO_2 [27]. The apparent (101) peaks of the TiO_2 (JCPDS card no. 84-1286) nanorods indicate anatase TiO_2. It is well known that the anatase TiO_2 exhibits a better photocatalytic activity than rutile TiO_2 [4]. Due to the presence of a ZnO/TiO_2 heterojunction, the recombination of electron-hole pairs will be restrained. This improves the availability of the electrons to transfer to the TiO_2 surface of the ZnO/TiO_2 nanorods and consequently causes a redox reaction [28].

In Figure 3, the PL spectra of the ZT-300, ZT-400, and ZT-500 show that the UV emission peak of the ZnO/TiO_2 nanorods appeared at 382 nm due to the recombination of free exciton [29, 30]. The peak of the ZT-500 was higher than those of other samples, implying that the crystallinity of the ZnO/TiO_2 nanorods was improved with increasing annealing temperature of the seed layers. A visible peak of the ZnO/TiO_2 nanorods appeared at 600 nm corresponding to

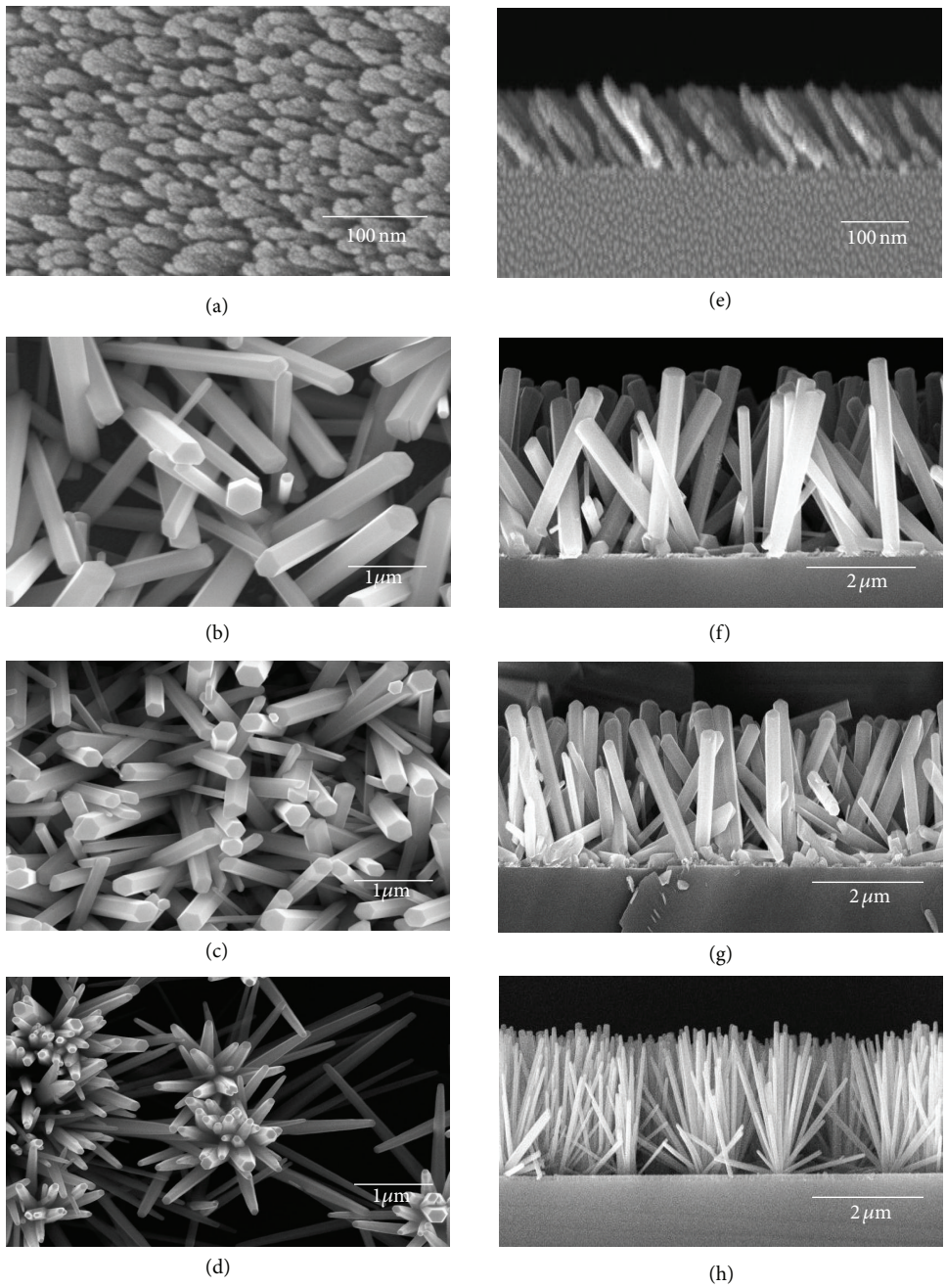

Figure 1: SEM images of the top view of (a) TiO_2 nanorods, (b) ZT-300, (c) ZT-400, and (d) ZT-500 and cross-sectional view of (e) TiO_2 nanorods, (f) ZT-300, (g) ZT-400, and (h) ZT-500.

the orange emission. It is related to the levels within band gap caused by defects, and in this case it is associated with oxygen vacancy defects [30]. The orange emission is due to the deep defects and it means that oxygen vacancy defects were deeply inserted in the band gap [31, 32]. The emission intensity of the ZnO/TiO_2 nanorods was enhanced with increasing annealing temperature of the seed layers. The inset of Figure 3 shows that the intensities of the visible peaks of the ZT-500 and Z-500 at 600 nm are greatly different. This implies that TiO_2 nanorods with ZnO seed layers annealed at 500°C work as supportive materials in the intense increase of orange emission in many ways [29]. The first thing is that they made the radius of ZnO nanorods reduce which is supported from SEM analysis in Figure 1. It leads to the increase of surface area active to the irradiating light and contribute to the increase of PL peak [33]. The second thing is to cause the increase of defects. Atomic diffusion between the ZnO and TiO_2 nanorods becomes vigorous at high temperature, resulting in the increase of defects [27]. A difference in the photocatalytic activity is related to the concentration of oxygen defects

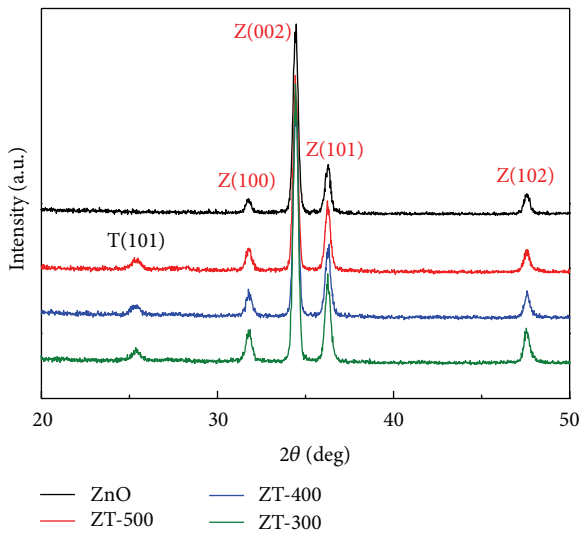

Figure 2: XRD patterns of ZT-300, ZT-400, ZT-500, and ZnO.

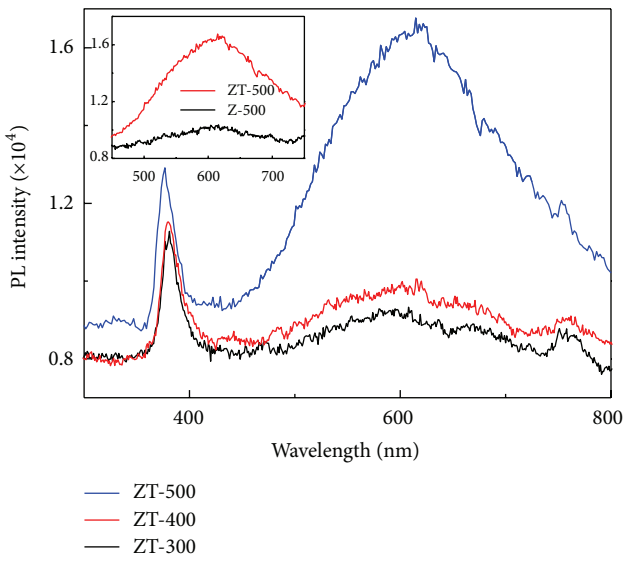

Figure 3: Room temperature PL spectra of ZT-300, ZT-400, and ZT-500. The inset shows visible emission of Z-500, and ZT-500.

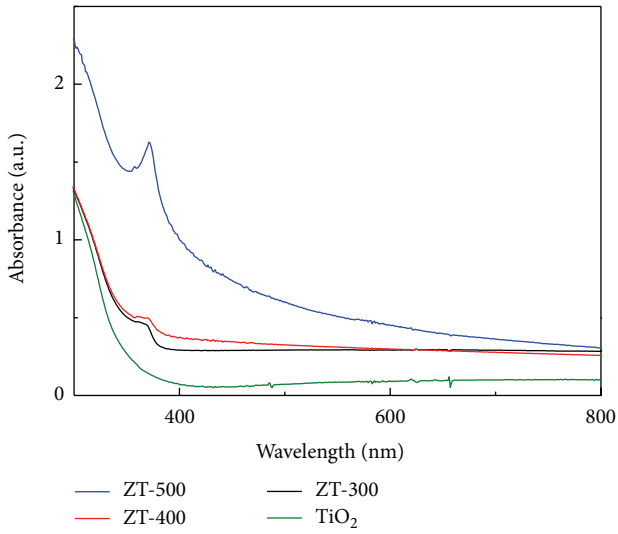

Figure 4: UV-vis absorbance spectra of ZT-300, ZT-400, ZT-500, and TiO_2.

on the surface layer as well as surface adsorption ability. The oxygen vacancy defects work as an electron acceptor and trap photogenerated electrons decreasing the surface recombination of electron-hole pairs. As described above, the oxygen vacancy and the interstitial oxygen defects promote separation of electron-hole pairs to minimize the electron recombination, leading to higher photocatalytic activity [30, 34, 35].

Figure 4 shows the UV-visible absorbance spectra of the ZT-300, ZT-400, and ZT-500. The absorption edge was observed to be located at 371 nm for the crystalline ZnO. The absorbance increased significantly with increasing the annealing temperature of the seed layers. It results from a large surface area of ZT-500 with flower structure composed of thin nanorods as shown in Figure 1. It is that the amorphous phase is reduced with increasing the seed layer annealing temperature since more energy is supplied for crystalline growth, thus resulting in an improvement in crystallinity of the ZT-500. The relationship of the absorption coefficient and the incident photon energy of ZnO and TiO_2 nanorods is given by the equation $\alpha(h\nu) \propto (h\nu - E_0)^n$, where α is the absorption coefficient, $h\nu$ is the energy of the incident photon, n is 0.5 for the semiconductor with direct band gap, and E_0 is value of energy gap [36]. According to the above equation, the band gap of the ZnO nanorods was determined as 3.22 eV and that of the TiO_2 nanorods as 3.19 eV.

The photocatalytic activities of the ZnO/TiO_2 and ZnO nanorods were evaluated by the degradation of the MB under the UV irradiation. Figure 5(a) shows the UV-visible absorption spectra of the MB for the ZT-500 with various UV irradiation times. The MB showed a major absorption band at 665 nm which became transparent after 120 min irradiation, resulting from facile destruction of the chromophoric structure of the MB [37].

The photocatalytic activity of the samples can be represented by a plot of C/C_o versus UV irradiation time [38]. Here C is the concentration at irradiation time t and C_o is the initial concentration. Figure 5(b) shows the photocatalytic activity of the ZnO/TiO_2 and ZnO nanorods by the photodegradation of the MB under the UV irradiation. The MB was decomposed by 76.2%, 83.3%, 87.0%, and 95.5% after 4 h of the UV irradiation for Z-500, ZT-300, ZT-400, and ZT-500, respectively. The samples with a heterojunction of the ZnO/TiO_2 nanorods showed an enhanced photocatalytic activity than the ZnO nanorods. Improved photocatalytic activity comes from a high surface area of the TiO_2 nanostructure [27], and coupling effect of ZnO and TiO_2, which increases interfacial charge transfer and decreases the recombination of the electrons and holes by promoting their separation [39–41]. The ZT-500 showed

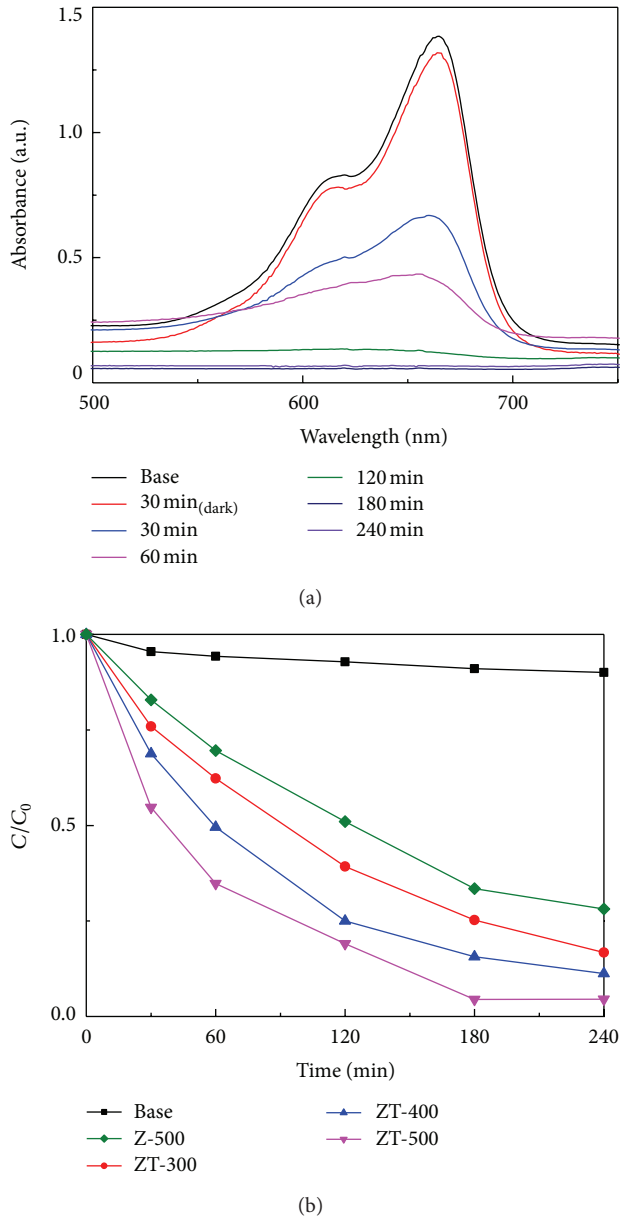

FIGURE 5: (a) UV-vis absorbance spectra of MB for the ZT-500. (b) Photodegradation of the MB for ZT-300, ZT-400, ZT-500, and Z-500.

the best photocatalytic activity, indicating that defects on the ZnO nanorods can act as a dominant factor for enhancing photocatalytic activity. In addition, the ZT-500 has a high surface area leading to high absorption ability compared with those of other samples and a high ability of the generating photoinduced electron-hole pairs [37].

Figure 6 shows the diagram of the band gap structure of the ZnO/TiO_2 nanorods. The photogenerated electrons transfer from the conduction band of ZnO to the conduction band of TiO_2. This leads to a decrease in the electron-hole pairs recombination by promoting their separation, and the lifetime of the charge carriers is increased [39, 40]. The charge separation increases the efficiency of the interfacial charge

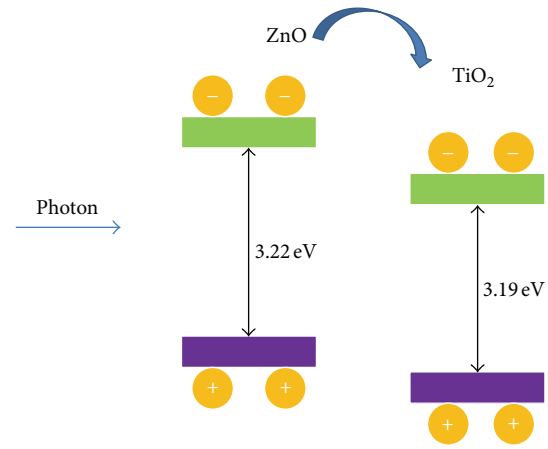

FIGURE 6: A schematic diagram of the electron and hole transfers for the ZnO/TiO_2 nanorods.

transfer and improves the redox process [40]. Therefore, the ZnO/TiO_2 nanorods have a strongly positive effect on the photocatalytic activity.

4. Conclusion

TiO_2 nanorod structure was prepared by electron-beam evaporation method through oblique beam incidence. ZnO seed layers were coated on TiO_2 and annealed at 300–500°C, which was followed by ZnO nanorod growth to form heterojunction structure of ZnO/TiO_2. The annealed ZnO seed layer was found to have a significant influence on the morphology of the ZnO/TiO_2 nanorod arrays. With increasing the annealing temperature of the ZnO seed layers, the size of the ZnO nanoparticles was gradually increased, leading to different morphology of ZT-500 composed of the thin nanorods which have a large surface area and a high absorption ability. The heterostructure of ZnO/TiO_2 can promote the separation of the electron-hole pairs and decrease their recombination enhancing photocatalytic reaction. When the annealing temperature of the seed layers reaches a relatively high temperature of 500°C, the atomic diffusion between the ZnO and TiO_2 nanorods is significantly enhanced, resulting in more interface defects which reduce the electron-hole recombination. As a result, ZnO/TiO_2 nanorods with high annealing temperature of the seed layers exhibited excellent photocatalytic activities for the decomposition of the MB.

Acknowledgments

This research was supported by the Human Resource Training Project for Regional Innovation (2012H1B8A2026179) and Basic Science Research Program (2012R1A1A4A010-15466) through the National Research Foundation of Korea (NRF) funded by the Ministry of Education Science and Technology (MEST).

References

[1] Y. Sun and M. N. R. Ashfold, "Photoluminescence from diameter-selected ZnO nanorod arrays," *Nanotechnology*, vol. 18, no. 24, Article ID 245701, 2007.

[2] M. Yang, G. Pang, L. Jiang, and S. Feng, "Hydrothermal synthesis of one-dimensional zinc oxides with different precursors," *Nanotechnology*, vol. 17, no. 1, pp. 206–212, 2006.

[3] J. Hu, T. W. Odom, and C. M. Lieber, "Chemistry and physics in one dimension: synthesis and properties of nanowires and nanotubes," *Accounts of Chemical Research*, vol. 32, no. 5, pp. 435–445, 1999.

[4] T. Kawahara, Y. Konishi, H. Tada, N. Tohge, J. Nishii, and S. Ito, "A patterned TiO_2(Anatase)/TiO_2(Rutile) bilayer-type photocatalyst: effect of the anatase/rutile junction on the photocatalytic activity," *Angewandte Chemie*, vol. 114, no. 15, pp. 2935–2937, 2002.

[5] K. S. Lee and I. S. Park, "Anatase-phase titanium oxide by low temperature oxidation of metallic Ti thin film," *Scripta Materialia*, vol. 48, no. 6, pp. 659–663, 2003.

[6] B. H. Kong and H. K. Cho, "Formation of vertically aligned ZnO nanorods on ZnO templates with the preferred orientation through thermal evaporation," *Journal of Crystal Growth*, vol. 289, no. 1, pp. 370–375, 2006.

[7] M. H. Huang, S. Mao, H. Feick et al., "Room-temperature ultraviolet nanowire nanolasers," *Science*, vol. 292, no. 5523, pp. 1897–1899, 2001.

[8] Y. Chen, D. M. Bagnall, H. J. Koh et al., "Plasma assisted molecular beam epitaxy of ZnO on c-plane sapphire: growth and characterization," *Journal of Applied Physics*, vol. 84, no. 7, pp. 3912–3918, 1998.

[9] R. S. Mane, W. J. Lee, H. M. Pathan, and S. H. Han, "Nanocrystalline TiO_2/ZnO thin films: fabrication and application to dye-sensitized solar cells," *Journal of Physical Chemistry B*, vol. 109, no. 51, pp. 24254–24259, 2005.

[10] Z. Zhang, Y. Yuan, Y. Fang, L. Liang, H. Ding, and L. Jin, "Preparation of photocatalytic nano-ZnO/TiO_2 film and application for determination of chemical oxygen demand," *Talanta*, vol. 73, no. 3, pp. 523–528, 2007.

[11] L. Xu, L. Shi, and X. Li, "Effect of TiO_2 buffer layer on the structural and optical properties of ZnO thin films deposited by E-beam evaporation and sol-gel method," *Applied Surface Science*, vol. 255, no. 5, pp. 3230–3234, 2008.

[12] Y. Xia, P. Yang, Y. Sun et al., "One-dimensional nanostructures: synthesis, characterization, and applications," *Advanced Materials*, vol. 15, no. 5, pp. 353–389, 2003.

[13] R. Calarco, M. Marso, T. Richter et al., "Size-dependent photoconductivity in MBE-grown GaN—nanowires," *Nano Letters*, vol. 5, no. 5, pp. 981–984, 2005.

[14] X. Liu, X. Wu, H. Cao, and R. P. H. Chang, "Growth mechanism and properties of ZnO nanorods synthesized by plasma-enhanced chemical vapor deposition," *Journal of Applied Physics*, vol. 95, no. 6, pp. 3141–3147, 2004.

[15] Z. W. Pan, Z. R. Dai, L. Xu, S. T. Lee, and Z. L. Wang, "Temperature-controlled growth of silicon-based nanostructures by thermal evaporation of SiO powders," *Journal of Physical Chemistry B*, vol. 105, no. 13, pp. 2507–2514, 2001.

[16] B. Cheng and E. T. Samulski, "Hydrothermal synthesis of one-dimensional ZnO nanostructures with different aspect ratios," *Chemical Communications*, vol. 10, no. 8, pp. 986–987, 2004.

[17] B. Liu and H. C. Zeng, "Hydrothermal synthesis of ZnO nanorods in the diameter regime of 50 nm," *Journal of the American Chemical Society*, vol. 125, no. 15, pp. 4430–4431, 2003.

[18] X. Y. Zhang, J. Y. Dai, H. C. Ong, N. Wang, H. L. W. Chan, and C. L. Choy, "Hydrothermal synthesis of oriented ZnO nanobelts and their temperature dependent photoluminescence," *Chemical Physics Letters*, vol. 393, no. 1–3, pp. 17–21, 2004.

[19] S. Baruah and J. Dutta, "Effect of seeded substrates on hydrothermally grown ZnO nanorods," *Journal of Sol-Gel Science and Technology*, vol. 50, no. 3, pp. 456–464, 2009.

[20] A. Sugunan, H. C. Warad, M. Boman, and J. Dutta, "Zinc oxide nanowires in chemical bath on seeded substrates: role of hexamine," *Journal of Sol-Gel Science and Technology*, vol. 39, no. 1, pp. 49–56, 2006.

[21] M. K. Hossain, S. C. Ghosh, Y. Boontongkong, C. Thanachayanont, and J. Dutta, "Growth of Zinc Oxide nanowires and nanobelts for gas sensing applications," *Journal of Metastable and Nanocrystalline Materials*, vol. 23, pp. 27–30, 2005.

[22] L. E. Greene, M. Law, J. Goldberger et al., "Low-temperature wafer-scale production of ZnO nanowire arrays," *Angewandte Chemie*, vol. 42, no. 26, pp. 3031–3034, 2003.

[23] J. Chung, J. Lee, and S. Lim, "Annealing effects of ZnO nanorods on dye-sensitized solar cell efficiency," *Physica B*, vol. 405, no. 11, pp. 2593–2598, 2010.

[24] M. Wang, E. J. Kim, J. S. Chung et al., "Influence of annealing temperature on the structural and optical properties of sol-gel prepared ZnO thin films," *Physica Status Solidi A*, vol. 203, no. 10, pp. 2418–2425, 2006.

[25] C. W. Zou, X. D. Yan, J. Han et al., "Preparation and enhanced photoluminescence property of ordered ZnO/TiO_2 bottlebrush nanostructures," *Chemical Physics Letters*, vol. 476, no. 1–3, pp. 84–88, 2009.

[26] N. Wang, C. Sun, Y. Zhao, S. Zhou, P. Chen, and L. Jiang, "Fabrication of three-dimensional ZnO/TiO_2 heteroarchitectures via a solution process," *Journal of Materials Chemistry*, vol. 18, no. 33, pp. 3909–3911, 2008.

[27] L. Xu, H. Shen, X. Li, and R. Zhu, "Influence of annealing temperature on the photoluminescence property of ZnO thin film covered by TiO_2 nanoparticles," *Journal of Luminescence*, vol. 130, no. 11, pp. 2123–2127, 2010.

[28] H. Y. Yang, S. F. Yu, S. P. Lau, X. Zhang, D. D. Sun, and G. Jun, "Direct growth of ZnO nanocrystals onto the surface of porous TiO_2 nanotube arrays for highly efficient and recyclable photocatalysts," *Small*, vol. 5, no. 20, pp. 2260–2264, 2009.

[29] J. H. Hyung, M. S. Akhtar, D. J. Kim, and S. K. Lee, "ZnO-nanowire-covered TiO_2 thin-film electrodes for improving the photovoltaic properties of dye-sensitized solar cells," *Journal of the Korean Physical Society*, vol. 55, no. 1, pp. 89–93, 2009.

[30] Y. Zheng, C. Chen, Y. Zhan et al., "Luminescence and photocatalytic activity of ZnO nanocrystals: correlation between structure and property," *Inorganic Chemistry*, vol. 46, no. 16, pp. 6675–6682, 2007.

[31] S. Parida, S. K. Rout, L. S. Cavalcante et al., "Structural refinement, optical and microwave dielectric properties of $BaZrO_3$," *Ceramics International*, vol. 38, no. 3, pp. 2129–2138, 2012.

[32] A. T. de Figueiredo, V. M. Longo, R. O. da Silva et al., "Structural XANES characterization of $Ca_{0.99}Sm_{0.01}TiO_3$ perovskite and correlation with photoluminescence emission," *Chemical Physics Letters*, vol. 544, pp. 43–48, 2012.

[33] A. E. Souza, G. T. A. Santos, B. C. Barra et al., "Photoluminescence of $SrTiO_3$: influence of particle size and morphology," *Crystal Growth & Design*, vol. 12, no. 11, pp. 5671–5679, 2012.

[34] J. Wang, P. Liu, X. Fu, Z. Li, W. Han, and X. Wang, "Relationship between oxygen defects and the photocatalytic property of zno nanocrystals in nafion membranes," *Langmuir*, vol. 25, no. 2, pp. 1218–1223, 2009.

[35] J. Lv, W. Gong, K. Huang et al., "Effect of annealing temperature on photocatalytic activity of ZnO thin films prepared by sol-gel method," *Superlattices and Microstructures*, vol. 50, no. 2, pp. 98–106, 2011.

[36] Z. Zhang, Y. Yuan, L. Liang, Y. Cheng, G. Shi, and L. Jin, "Preparation and photoelectrocatalytic activity of ZnO nanorods embedded in highly ordered TiO_2 nanotube arrays electrode for azo dye degradation," *Journal of Hazardous Materials*, vol. 158, no. 2-3, pp. 517–522, 2008.

[37] D. Chen, H. Zhang, S. Hu, and J. Li, "Preparation and enhanced photoelectrochemical performance of coupled bicomponent ZnO-TiO_2 nanocomposites," *Journal of Physical Chemistry C*, vol. 112, no. 1, pp. 117–122, 2008.

[38] L. Palmisano, M. Schiavello, A. Sclafani, C. Martin, I. Martin, and V. Rives, "Surface properties of iron-titania photocatalysts employed for 4-nitrophenol photodegradation in aqueous TiO_2 dispersion," *Catalysis Letters*, vol. 24, no. 3-4, pp. 303–315, 1994.

[39] M. A. Kanjwal, N. A. M. Barakat, F. A. Sheikh, S. J. Park, and H. Y. Kim, "Photocatalytic activity of ZnO-TiO_2 hierarchical nanostructure prepared by combined electrospinning and hydrothermal techniques," *Macromolecular Research*, vol. 18, no. 3, pp. 233–240, 2010.

[40] X. Yan, C. Zou, X. Gao, and W. Gao, "ZnO/TiO_2 core-brush nanostructure: processing, microstructure and enhanced photocatalytic activity," *Journal of Materials Chemistry*, vol. 22, pp. 5629–5640, 2012.

[41] M. Zhang, T. An, X. Liu, X. Hu, G. Sheng, and J. Fu, "Preparation of a high-activity ZnO/TiO_2 photocatalyst via homogeneous hydrolysis method with low temperature crystallization," *Materials Letters*, vol. 64, no. 17, pp. 1883–1886, 2010.